

On the use of explicitly correlated treatment methods for the generation of accurate polyatomic –He/H₂ interaction potential energy surfaces: The case of C₃–He complex and generalization

M. M. Al Mogren, O. Denis-Alpizar, D. Ben Abdallah, T. Stoecklin, P. Halvick, M.-L. Senent, and M. Hochlaf

Citation: *The Journal of Chemical Physics* **141**, 044308 (2014); doi: 10.1063/1.4890729

View online: <http://dx.doi.org/10.1063/1.4890729>

View Table of Contents: <http://scitation.aip.org/content/aip/journal/jcp/141/4?ver=pdfcov>

Published by the [AIP Publishing](#)

Articles you may be interested in

[Rovibrational energy transfer in the He-C₃ collision: Potential energy surface and bound states](#)

J. Chem. Phys. **140**, 084316 (2014); 10.1063/1.4866839

[Properties of the B⁺-H₂ and B⁺-D₂ complexes: A theoretical and spectroscopic study](#)

J. Chem. Phys. **137**, 124312 (2012); 10.1063/1.4754131

[A new ab initio intermolecular potential energy surface and predicted rotational spectra of the Ne-H₂S complex](#)

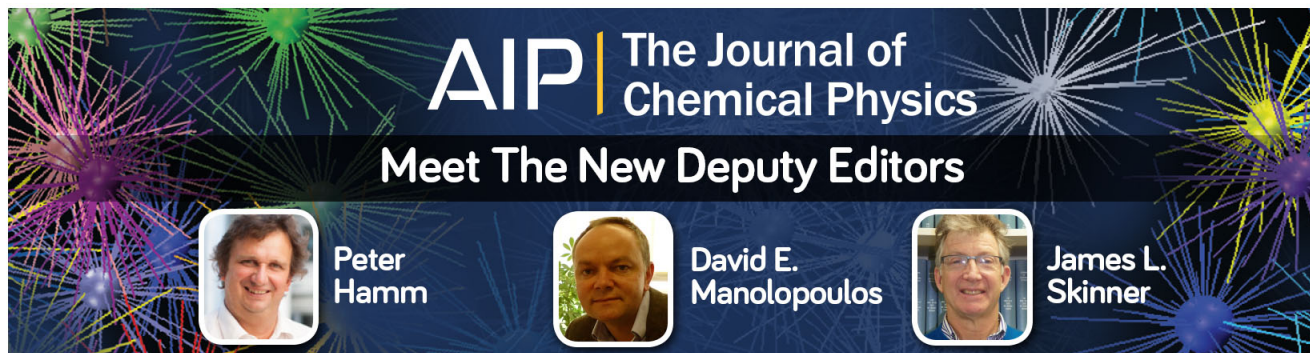
J. Chem. Phys. **136**, 214307 (2012); 10.1063/1.4725715

[Interaction-induced dipoles of hydrogen molecules colliding with helium atoms: A new ab initio dipole surface for high-temperature applications](#)

J. Chem. Phys. **136**, 044320 (2012); 10.1063/1.3676406




[The He-LiH potential energy surface revisited. II. Rovibrational energy transfer on a three-dimensional surface](#)

J. Chem. Phys. **122**, 074308 (2005); 10.1063/1.1851495



AIP | The Journal of
Chemical Physics

Meet The New Deputy Editors

	Peter Hamm		David E. Manolopoulos		James L. Skinner
---	-------------------	---	------------------------------	---	-------------------------

On the use of explicitly correlated treatment methods for the generation of accurate polyatomic –He/H₂ interaction potential energy surfaces: The case of C₃–He complex and generalization

M. M. Al Mogren,¹ O. Denis-Alpizar,^{2,3} D. Ben Abdallah,⁴ T. Stoecklin,² P. Halvick,² M.-L. Senent,⁵ and M. Hochlaf^{6,a)}

¹Chemistry Department, Faculty of Science, King Saud University, P.O. Box 2455, Riyadh 11451, Kingdom of Saudi Arabia

²Université de Bordeaux, ISM, CNRS UMR 5255, 33405 Talence Cedex, France

³Departamento de Física, Universidad de Matanzas, Matanzas 40100, Cuba

⁴Laboratoire de Spectroscopie Atomique, Moléculaire et Applications – LSAMA Université de Tunis, Tunisia and Department of General Studies, Riyadh Corporation of Technology, Technical and Vocational Training Corporation, P.O. Box: 42826, Riyadh 11551, Kingdom of Saudi Arabia

⁵Departamento de Química y Física Teóricas, Instituto de Estructura de la Materia, IEM-C.S.I.C., Serrano 121, Madrid 28006, Spain

⁶Université Paris-Est, Laboratoire Modélisation et Simulation Multi Echelle, MSME UMR 8208 CNRS, 5 bd Descartes, 77454 Marne-la-Vallée, France

(Received 15 May 2014; accepted 8 July 2014; published online 25 July 2014)

Through the study of the C₃($\tilde{X}^1\Sigma_g^+$) + He(¹S) astrophysical relevant system using standard (CCSD(T)) and explicitly correlated (CCSD(T)-F12) coupled cluster approaches, we show that the CCSD(T)-F12/aug-cc-pVTZ level represents a good compromise between accuracy and low computational cost for the generation of multi-dimensional potential energy surfaces (PESs) over both intra- and inter-monomer degrees of freedom. Indeed, the CCSD(T)-F12/aug-cc-pVTZ 2D-PES for linear C₃ and the CCSD(T)-F12/aug-cc-pVTZ 4D-PES for bent C₃ configurations gently approach those mapped at the CCSD(T)/aug-cc-pVXZ (X = T,Q) + bond functions level, whereas a strong reduction of computational effort is observed. After exact dynamical computations, the pattern of the rovibrational levels of the intermediate C₃–He complex and the rotational and rovibrational (de-) excitation of C₃ by He derived using both sets of PESs agree quite well. Since C₃ shows a floppy character, the interaction PES is defined in four dimensions to obtain realistic collisional parameters. The C–C–C bending mode, which fundamental lies at 63 cm⁻¹ and can be excited at very low temperatures is explicitly considered as independent coordinate. Our work suggests hence that CCSD(T)-F12/aug-cc-pVTZ methodology is the key method for the generation of accurate polyatomic – He/H₂ multi-dimensional PESs. © 2014 AIP Publishing LLC. [<http://dx.doi.org/10.1063/1.4890729>]

I. INTRODUCTION

Small carbon clusters, C_n, play an important role in our environment, as precursors of soot and large carbon molecules, including aromatic species and fullerenes, and also in Astrochemistry. The tricarbon cluster, C₃,¹ is considered as the most abundant chain in the interstellar medium (ISM). Its first spectroscopic observation in one astrophysical source was reported over a century ago when Huggins investigated the spectra of a comet tail and identified the emission of C₃ through the $\tilde{A}^1\Pi_u$ - $\tilde{X}^1\Sigma_g^+$ band. In 1988, the same emission was observed in cold carbon stars and supergiant circumstellar shells.² Because of its importance, considerable theoretical and experimental work was devoted to C₃ in the ground ($\tilde{X}^1\Sigma_g^+$) and electronically excited ($\tilde{A}^1\Pi_u$, $\tilde{a}^3\Pi_u$, $\tilde{b}^3\Pi_g$, $^1\Sigma_u^+$) states.^{3–5} The $\tilde{A}^1\Pi_u$ - $\tilde{X}^1\Sigma_g^+$ system has been extensively studied in laboratory.^{2,6–8} The first electronically excited state $\tilde{A}^1\Pi_u$, which lies ~ 3 eV over the ground state,

presents a linear geometry and exhibits large Renner-Teller effects.⁹ In the singlet manifold, $^1\Sigma_u^+$ represents the next higher electronically excited state. The $^1\Sigma_u^+$ - $\tilde{X}^1\Sigma_g^+$ pattern was observed and studied by Chang and Graham in the 1980s,¹⁰ which was confirmed by a recent vacuum ultraviolet spectroscopy study on the matrix-isolated C₃ molecule.¹¹ The observation of this band is difficult because of the strong interaction with the $\tilde{A}^1\Pi_u$ state and because of interactions with the triplet manifold. Two metastable triplet states, $\tilde{a}^3\Pi_u$ and $\tilde{b}^3\Pi_g$, have been detected in matrix and gas phase.^{11,12} The $\tilde{b}^3\Pi_g$ state is less known, even though gas phase $\tilde{b}^3\Pi_g$ - $\tilde{a}^3\Pi_u$ vibronic transitions have been observed.^{13,14} However, as has been shown in experimental matrix isolated studies of C₃^{11,12,15} both manifolds interact mutually. For interpretation, several potential energy surfaces (PESs)^{5,16–18} were generated for the ground and excited states of C₃. In whole, this huge amount of experimental and theoretical investigations led to accurate characterization and to a reliable set of spectroscopic data for C₃($\tilde{X}^1\Sigma_g^+$). They also showed that this molecule presents a pronounced floppy character.

^{a)} Author to whom correspondence should be addressed. Electronic mail: ho-chlaf@univ-mlv.fr. Phone: +33 1 60 95 73 19. FAX: +33 1 60 95 73 20.

More recently, the Herschel mission and ALMA telescopes have specific observations for C_3 . These observations provided and still provide huge amount of data in the far-infrared and submillimeter energy domains for this molecule. The accurate analysis of this highly resolved spectra needs, in addition to high quality spectroscopic studies, the computations of cross sections for the excitation and de-excitation of $C_3(\tilde{X}^1\Sigma_g^+)$ by collisions with the abundant H_2 molecule. For simplicity, H_2 is replaced here by He, sure less abundant, but presenting similar electronic structure. For many systems, the similarity of collisional properties computed with He and para- H_2 has been demonstrated (see, for instance, Refs. 19, 20. Rate constants for rotational (de-)excitation of $C_3(\tilde{X}^1\Sigma_g^+)$ by He (1S) were computed for the first time, in 2008, by Ben Abdallah *et al.*,²¹ after incorporation of a 2D interaction PES into full close-coupling quantum scattering calculations within the rigid monomer approximation (RMA). The 2D-PES was generated at the CCSD(T)/aug-cc-pVTZ + 3s3p2d1f bond functions (denoted hereafter as 2D-BA) and it was developed over R (distance between this center of mass and the He atom, Figure 1) and θ (defining the rotation of He around C_3 , Figure 1) Jacobi coordinates, where the C_3 molecule was kept fixed to its structure at the ground vibrational state ($r_0 = 1.2772 \text{ \AA}$,^{22,23} i.e., linear C_3 bond distances). The collision rates were obtained for low-temperatures ($5 \text{ K} \leq T \leq 15 \text{ K}$) avoiding hence to reach the first bending anharmonic level of C_3 (located at very low energy, 63 cm^{-1}).

In 2009, Zhang *et al.*²⁴ provided two 2D-PESs of C_3 -He complex both of them computed at the MP4 and CCSD(T) levels. These 2D PESs were mapped along the R, θ Jacobi coordinates. C_3 structure was frozen to be either linear ($CCC = 180^\circ$) or bent ($CCC = 160^\circ$). Thus, they found that the two global minima correspond to a slightly distorted T-shaped configuration. Using these 2D PESs, these authors derived the rovibrational levels of C_3 -He complex. Very recently, Denis-Alpizar *et al.*²⁵ built a 4D-PES over the R, θ Jacobi coordinates and also over the azimuthal angle (ϕ) and the

bending angle (γ) of the C_3 molecule (Figure 1). The intramonomer C-C distances were kept fixed to their r_0 experimental value in $C_3(\tilde{X}^1\Sigma_g^+)$. The electronic computations were carried out using the standard coupled-cluster technique with single and double excitations and a perturbative treatment of triple excitations (CCSD(T)) in connection with the aug-cc-pVQZ basis set and mid-bond functions. These larger computations confirm the near T-shaped structure of the C_3 -He. These 4D-PES was used for the deduction of C_3 -He bound states including excitations for the C_3 bending motion. In the following, we will refer to this PES as 4D-DA.

In this paper, we use the explicitly correlated coupled cluster methodology (CCSD(T)-F12) to generate two vdW surfaces corresponding to the ground electronic states: one 2D-PES for linear- C_3 ($C-C-C = 180^\circ$) interacting with He and one 4D-PES for the C_3 -He system over the van der Waals (vdW) inter monomer coordinates and the internal bending coordinate. Both PESs correlate to the $C_3(\tilde{X}^1\Sigma_g^+) + He(^1S)$ in the asymptote region. For the 2D-PES (4D-PES), we use a similar coordinate system and an analytical fitting procedure than Ben Abdallah *et al.*²¹ and Denis-Alpizar *et al.*,²⁵ which allows direct comparison of our explicitly correlated PESs with those deduced using the standard coupled cluster techniques. After dynamical computations, we also compare the pattern of bound rovibrational levels of this complex derived using both sets of PESs and the cross sections for the (de-)excitation of C_3 by He. This is the first time where the use of explicitly correlated methods for the generation of multidimensional potentials for vdW systems depending on both intra- and intermolecular degrees of freedom. As has been recently established for C_4 -He, HCl-He, and CO_2 - CO_2 complexes,²⁶⁻²⁸ an overall agreement together with a strong reduction on computational time and disk occupancy are found when CCSD(T)-F12 in connection with the aug-cc-pVTZ basis set is used. Hence, it represents the selected method for mapping of multidimensional PESs of polyatomic - He/ H_2 vdW interacting systems.

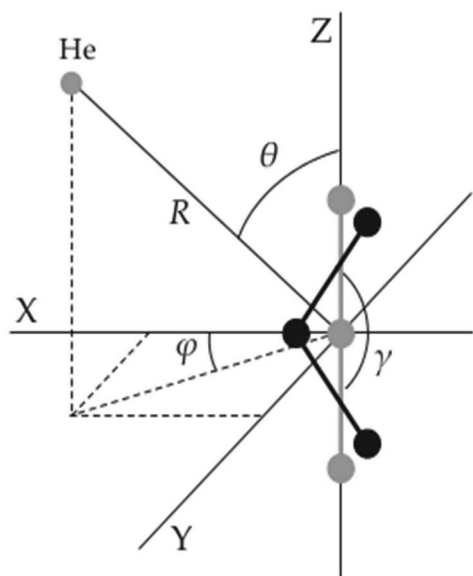


FIG. 1. Coordinate system of the C_3 -He complex. The linear C_3 molecule is along the Z axis, and the bent C_3 molecule is in the plane XZ.

II. GENERATION OF THE 2D AND 4D PES AND ANALYTICAL FITS

The electronic structure computations were performed with the MOLPRO (version 2012) program suite²⁹ in the C_1 point group. They were carried out with the explicitly-correlated (CCSD(T)-F12) method in connection with the augmented correlation-consistent aug-cc-pVTZ basis set. We followed the methodology established by Hochlaf and co-workers for the computations of accurate interaction potentials for vdW systems.²⁶⁻²⁸ Briefly, the C and He atoms were described using the aug-cc-pVTZ Dunning and co-workers' basis set^{30,31} using the corresponding auxiliary basis sets and density fitting functions,^{32,33} which correspond to the default basis sets, CABS(OptRI) as implemented in MOLPRO. As widely documented in the literature,³⁴⁻³⁶ approximations *a* or *b* in explicitly correlated CCSD(T)-F12 computations lead to similar vdW potentials except a global shift of the total energies is observed.³⁴⁻³⁶ Hence, one may use approximations *a* or *b*. For this paper, we used the approximation *a*, which we will refer hereafter as CCSD(T)-F12. Nevertheless, we

TABLE I. Comparison between present and previous minima characteristics for selected C_3 -He configurations. Distances (R) are in bohr, angles (θ , ϕ , and γ) are in degrees and potentials (V) are in cm^{-1} .

Method/basis set	Linear C_3 ($\gamma = 180^\circ$)			Bent C_3 ($\gamma = 160^\circ$)				Bent C_3 ($\gamma = 120^\circ$)			
	R	θ	V	R	θ	ϕ	V	R	θ	ϕ	V
CCSD(T)-F12/aug-cc-pVTZ ^a	6.78	83.5	-27.91	6.61	90	180	-31.18	6.58	90	180	-36.96
CCSD(T)/aug-cc-pVQZ + mid-bond functions ^b	6.82	81.4	-26.73	6.64	90	180	-29.90	6.57	90	180	-36.30
CCSD(T)/aug-cc-pVTZ + 3s3p2d1f ^c	6.75	90	-25.87
MP4/C:cc-pVTZ and He:aug-cc-pVTZ ^d	6.65	90	-31.29
CCSD(T)/aug-cc-pVTZ/3s3p2d ^d	6.78	90	-25.54	6.84	0	...	-27.66

^a4D-F12 PES. This work.^b4D-DA PES. Reference 25.^c2D-BA PES. Reference 21.^d2D PES. Reference 24.

needed to correct for the non-size-consistency of CCSD(T)-F12 caused by the inclusion of triples, since CCSD-F12 itself is size-consistent.^{26,27,37-40} Therefore, the total energies were shifted up by their corresponding values for $R = 100$ bohrs (of $\sim 4.5 \text{ cm}^{-1}$). This forces hence the PES to decay to zero in the asymptotic region.

When determining the interaction potentials ($V(R, \theta, \gamma, \phi)$), we took into account the basis set superposition error (BSSE) using the Boys and Bernardi counterpoise correction formula⁴¹

$$V(R, \theta, \gamma, \phi) = E_{C_3-\text{He}}(R, \theta, \gamma, \phi) - E_{C_3}(R, \theta, \gamma, \phi) - E_{\text{He}}(R, \theta, \gamma, \phi), \quad (1)$$

where $E_{C_3-\text{He}}(R, \theta, \gamma, \phi)$, $E_{C_3}(R, \theta, \gamma, \phi)$, and $E_{\text{He}}(R, \theta, \gamma, \phi)$ are the energies of C_3 -He, C_3 , and He. These energies were computed in the full basis set of the C_3 -He complex. Close to the C_3 -He equilibrium, the contribution of the BSSE to the interaction energy was about 1%–2%.

More than 24 700 total energies were carried out for different nuclear configurations covering the equilibrium geometry and the regions of the interactions of He with C_3 . The θ angle was varied from 0° to 90° by step of 10° , and ϕ from 0° to 180° by step of 30° . The grids on γ and R were not uniform. Indeed, γ was set to all values from 30° to 180° by step of 10° , γ was also fixed to 175° to account for the quasilinear behavior of C_3 along this coordinate. For R coordinate, we considered 29 values ($R = 4.1, 4.2, 4.3, 4.4, 4.5, 4.6, 4.8, 5.0, 5.2, 5.6, 6.0, 6.5, 7.0, 7.5, 8.0, 9.0, 10.0, 11.0, 12.0, 13.0, 14.0, 15.0, 16.0, 17.0, 18.0, 19.0, 20.0, 22.0$, and 100, in bohrs).

Later on, the CCSD(T)-F12/aug-cc-pVTZ total energies were used to deduce a 2D (denoted hereafter as 2D-F12) and 4D (denoted as 4D-F12) analytical representations for C_3 -He. For 2D-F12, we followed the methodology of Ben Abdallah *et al.*²¹ This was developed over the R and θ Jacobi coordinates where the γ and ϕ were kept fixed to 180° and 0° (linear C_3) and fitted using a Legendre polynomial expansion. For 4D-F12, we used the fitted procedure described by Denis-Alpizar *et al.*²⁵ Briefly, $V(R, \theta, \gamma, \phi)$ is deduced as the contribution of short- and long-range terms. Both of them are developed over normalized associated Legendre polynomials depending on θ and Fourier transform functions depending on ϕ . The coefficients of this expansion are function of R and γ . The switch between the short and long range terms is ensured

by a switching function, S, which is a function of R. Further details can be found in Ref. 25.

For both fits, the mean difference between the analytic fit and the *ab initio* interaction energies was less than 3.8% over the corresponding entire grid. This mean relative error should only be slightly overestimated. Indeed, several precautions were taken in order to avoid regions of the grid (at very long ranges and at the limit between attractive and repulsive regions at short range) where the potential is zero. Both expansions can be sent upon request.

III. RESULTS AND DISCUSSION

Table I presents the complex properties corresponding to the linear ($\gamma = 180^\circ$) and bent structures ($\gamma = 160^\circ$ and 120°) deduced from 2D-BA, 4D-DA, 4D-F12, as well as, those derived from the 2D-PESs of Zhang *et al.*²⁴ Figures 2 and 3 display two-dimensional cuts of the C_3 -He 4D-F12 PES together with the corresponding 2D cuts deduced from 4D-DA PES. These cuts are done over the R Jacobi distance and intra- and the inter-monomer bending coordinates. At first glance, both sets of contour plots are similar. For linear C_3 , 2D-DA, our 2D-F12 and the one derived from 4D-DA PESs are similar. In addition, the anisotropy of the PES along the R, θ , ϕ , and γ already noticed by Denis-Alpizar *et al.*²⁵ is well reproduced by the CCSD(T)-F12/aug-cc-pVTZ method. In the following, we will concentrate on the small deviations observed between 4D-F12 and 4D-DA.

For linear C_3 configuration ($\gamma = 180^\circ$), the minimum of the 4D-F12 PES is -27.91 cm^{-1} and corresponds to $\theta = 83.5^\circ$ and $R = 6.78 a_0$. In the 4D-DA PES, the minimum of -26.73 cm^{-1} is located at $R = 6.82 a_0$ and $\theta = 81.4^\circ$. In both cases, the barrier between the two symmetric minima is very small: it has been computed to be 0.03 cm^{-1} with CCSD(T)-F12/aug-cc-pVTZ, while it was found to be 0.07 cm^{-1} with the standard coupled cluster approach. It is worth noting that these values are in the order of the RMS. Nevertheless the *ab initio* points confirm that the minimum is not exactly for $\theta = 90^\circ$. For $\gamma = 180^\circ$, Zhang *et al.*²⁴ computed a relatively deep potential by using MP4, which is rather doubtful. This was corrected well in their CCSD(T) treatment which is consistent with the present findings.

As expected, both PESs show similar behaviors along the inter-monomer coordinates and along the γ C_3 internal

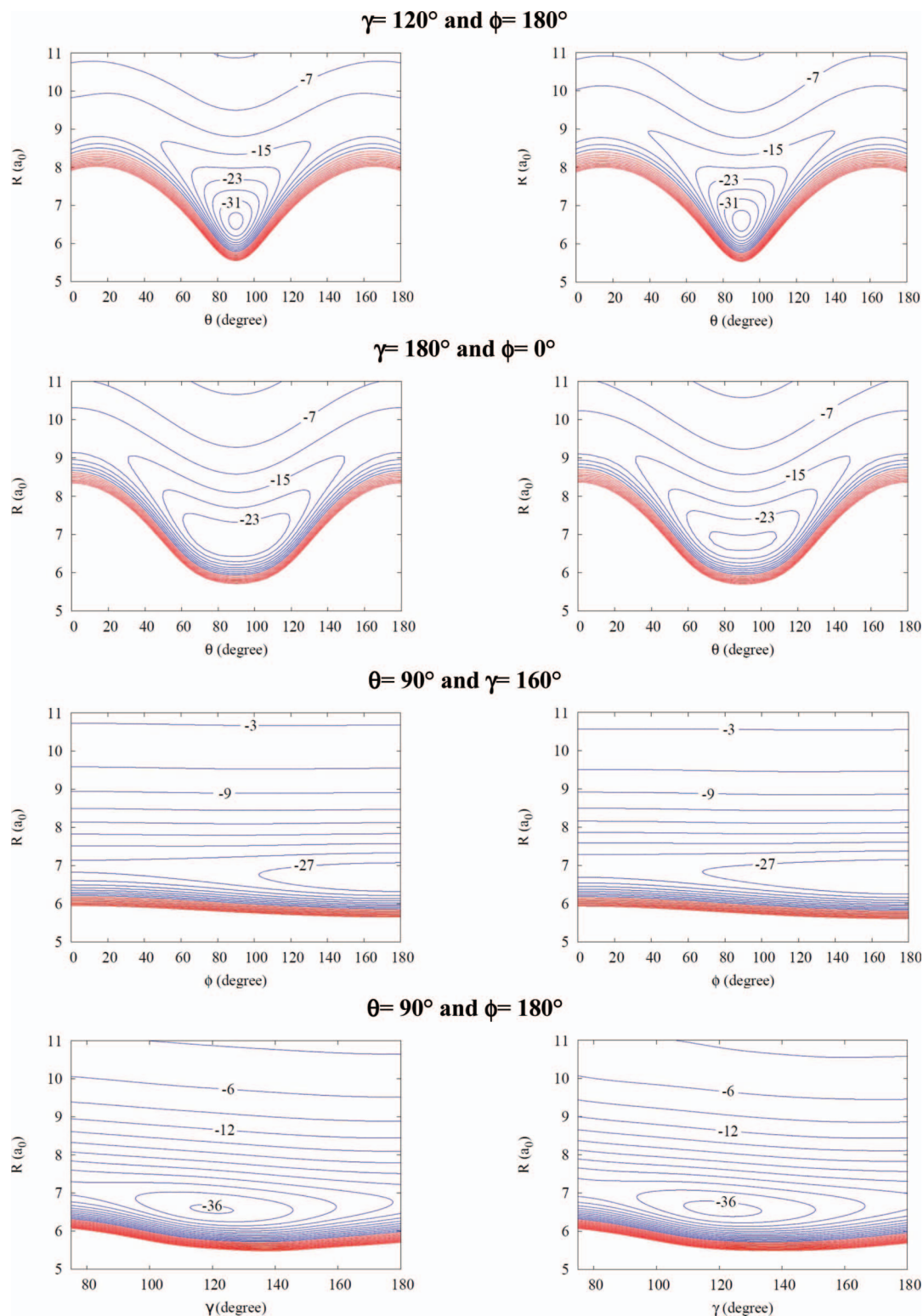


FIG. 2. Contour plots of the C_3 -He PES (in cm^{-1}) along the R and internal and intra-bending coordinates calculated using the CCSD(T)/aug-cc-pVQZ+mid bound function method (4D-DA PES, left) and at the CCSD(T)-F12/aug-cc-pVTZ level (4D-F12 PES, right). Here the intramolecular CC distances are fixed to r_0 values. The zero of energy is taken as that of the $C_3(\tilde{X}^1\Sigma_g^+) + \text{He}(^1S)$ asymptote.

bending. For $\gamma = 180^\circ$, 4D-F12 is $\sim 1.2 \text{ cm}^{-1}$ deeper. This result unnoticed in the CCSD(T) surfaces, derives from the fact that explicitly correlated methods account better for electron correlation. Generally, CCSD(T)-F12/aug-cc-pVTZ results are viewed to be as accurate as those computed using

CCSD(T)/aug-cc-pV5Z.²⁷ This makes the system dissociation energy (from the first calculation of the bound levels) 0.4 cm^{-1} deeper with respect to Denis-Alpiza *et al.*²⁵ calculation (see below). Explicitly correlated treatment leads also to near T-shape equilibrium structure for the C_3 -He complex very

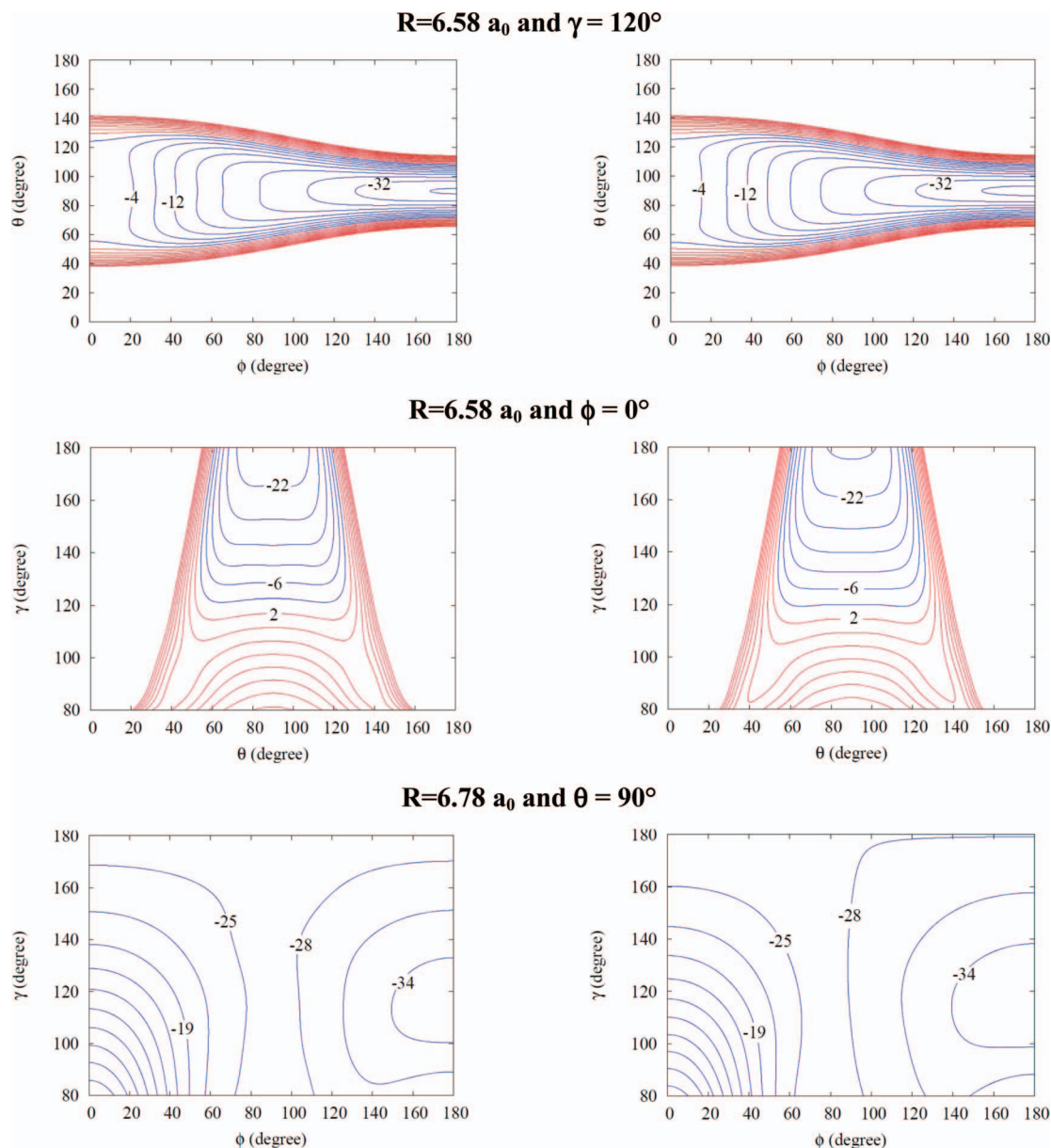


FIG. 3. Contour plots of the C_3 -He PES (in cm^{-1}) along the internal and intra-bending coordinates calculated using the CCSD(T)/aug-cc-pVQZ+mid bound function method (4D-DA PES, left) and at the CCSD(T)-F12/aug-cc-pVTZ level (4D-F12, right). Here the intramolecular CC distances are fixed to r_0 values. The zero of energy is taken as that of the $C_3(\tilde{X}^1\Sigma_g^+) + \text{He}(^1S)$ asymptote.

close to the one found by these authors. Indeed, we compute $R = 6.59$ bohrs, $\theta = 90^\circ$, $\gamma = 120^\circ$, and $\phi = 180^\circ$ at equilibrium that compare quite well with their equilibrium geometry, i.e., $R = 6.57$ bohrs, $\theta = 90^\circ$, $\gamma = 120^\circ$, and $\phi = 180^\circ$. The 4D-F12 potential depth is -37.1 cm^{-1} , which is slightly deeper than the depth of the 4D-DA PES (-36.3 cm^{-1}). Hence, both PESs are similar, whereas the computational time (CPU time) using explicitly correlated method is reduced by ~ 2 orders of magnitude and the disk occupancy is reduced by a factor of ~ 40 .

IV. APPLICATIONS

A. Bound states computations

The calculations of the bound levels were done using the atom-rigid bender close coupling (RB-CC) approach

presented recently by Stoecklin *et al.*⁴² We took advantage of the fact that the bound states calculations differ from the scattering calculations only in the boundary conditions. A modification in our scattering code based on the log-derivative propagator following the recommendations of Hutson and Thornley⁴³ was introduced to compute the ro-vibrational levels of C_3 -He complex using the 4D-DA PES. The details of these calculations were described in Ref. 25. Let us recall here only some of the essential features. For instance, we computed the rovibrational energies and wavefunctions of the rigid bender C_3 molecule using the symmetry adapted Hamiltonian developed by Carter *et al.*⁴⁴ The close coupling equations were written considering the bending-rotation interaction. The calculations using the 4D-F12 PES were performed for two values of the propagator step size (0.05 bohr and 0.1 bohr), and the values of the bound state

TABLE II. Energies (E in cm^{-1}) of the bound states of $\text{C}_3\text{-He}$ complex. J and p are the rotational quantum numbers and the parity of the levels, respectively. See Ref. 25 for more details.

J	p	E^a	E^b	E^c
0	+	-10.14	-9.73	-7.59
0	+	-4.43
0	+	-3.03	-3.00	-2.10
1	+	-3.75	-3.63	...
1	-	-9.65	-9.26	...
1	-	-4.18	-4.08	...
1	-	-2.27	-2.22	...
2	+	-8.74	-8.35	...
2	+	-7.59	-7.18	...
2	+	-3.70	-3.61	...
2	+	-1.04	-0.98	...
2	-	-7.62	-7.20	...
2	-	-2.66	-2.54	...
3	+	-6.31	-5.92	...
3	+	-1.06	-0.95	...
3	-	-7.47	-7.09	...
3	-	-6.17	-5.81	...
3	-	-2.76	-2.68	...
4	+	-5.92	-5.55	...
4	+	-4.22	-3.92	...
4	+	-1.44	-1.26	...
4	+	-1.34	-1.02	...
4	-	-4.58	-4.23	...
4	-	-1.42	-1.01	...
5	+	-2.45	-2.13	...
5	-	-4.08	-3.74	...
5	-	-1.84	-1.62	...
6	+	-1.95	-1.64	...

^a4D-F12 PES. This work.

^b4D-DA PES of Ref. 25.

^c2D-PES of Ref. 24.

energies were obtained from a Richardson extrapolation. We included in the calculations six bending eigenfunctions of C_3 and ten rotational eigenfunctions for each bending function. The maximum propagation distance was set to be 50 bohrs.

Table II presents the bound state energies of the He-C_3 complex. The total angular momentum J and the parity ϵ are also reported. We give also the values reported by Denis-Alpizar *et al.*,²⁵ using the RB-CC and those of Zhang *et al.*²⁴ considering the C_3 as a linear rigid molecule. The maximum value of the total angular momentum J leading to bound states is 6. Since the $\nu_2 = 0 \rightarrow \nu_2 = 1$ excitation energy of C_3 ($\sim 63 \text{ cm}^{-1}$) is larger than the depth well of the interaction potential, all the He-C_3 bound levels correspond to the bending quantum number of C_3 $\nu_2 = 0$. This PES supports 27 bound levels and the dissociation energy (D_e) is 10.14 cm^{-1} , which is 0.41 cm^{-1} higher than the calculated D_e from the 4D-DA PES. In fact, all our values are smaller than the computed ones using the 4D-DA PES, since our PES is expected to consider more correlation. The difference of the number of levels for $J = 0$ between our calculations and those of Zhang *et al.*²⁴ arises from symmetry restraints as Denis-Alpizar *et al.*²⁵ have discussed.

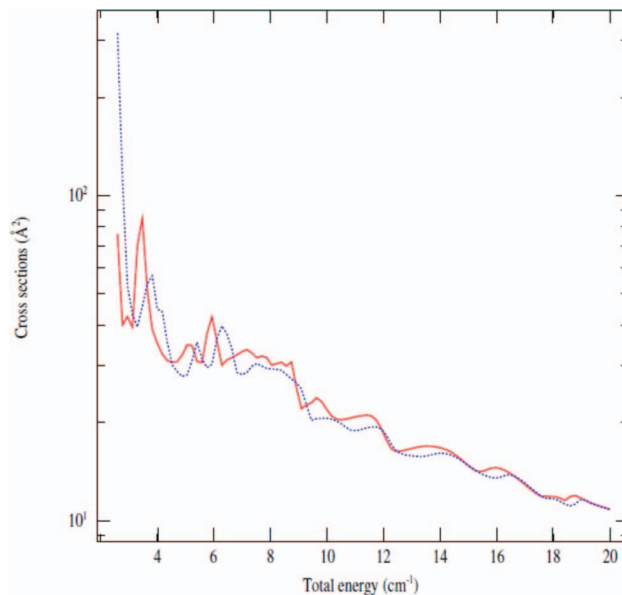


FIG. 4. Inelastic excitation close-coupling cross sections for $\text{C}_3(\tilde{X}^1\Sigma_g^+)$ in collision with $\text{He}(^1S)$, as a function of kinetic energy for the $J = 2 \rightarrow 0$ transition computed using either 2D-F12 (red curve) or 2D-BA PESs of Ref. 21 (blue curve).

B. Cross sections calculations

The analytical representations of the 2D-PESs were used for computing the cross sections corresponding to the low energy collision rotational excitations of C_3 by He. These computations have been performed using the CC approach. Since CC is numerically exact, the results reflect the quality of the PESs incorporated into these calculations. Figure 4 presents the inelastic cross sections for the $J = 2 \rightarrow 0$ transitions computed using 2D-BA and 2D-F12. Mostly, no obvious significant differences exist between the two sets of data signature of the agreement between the cross sections obtained using both PESs.

In order to check the effect of the differences between the 4D-F12 PES and the surface of Denis-Alpizar *et al.*

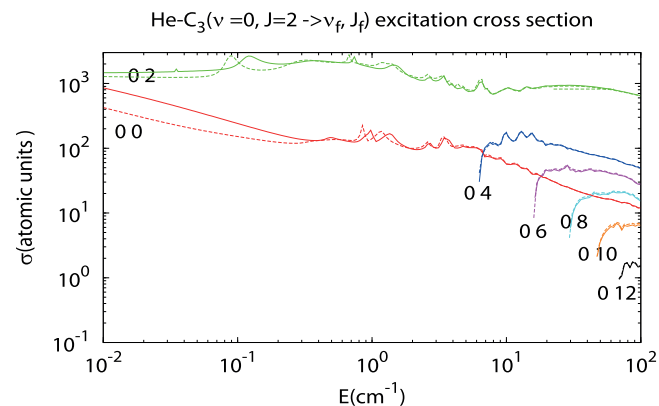


FIG. 5. Comparison of the elastic and excitation RB-CC cross section of $\text{C}_3(\nu = 0, j = 2)$ in collisions with He as a function of collision energy using two different PESs. The results obtained with the PES of Denis-Alpizar *et al.* (4D-DA²⁵) are represented by lines, while those obtained with the present 4D-F12 surface are represented by dashed lines. The final level is indicated by two integers designating the bending and the rotational quantum numbers.

(4D-DA) on the dynamics of the He–C₃ collision, we performed dynamics calculation using the Rigid Bender Close Coupling method (RBCC).⁴² This method allows treating exactly the coupling between bending and rotation within the rigid bender approximation. All the details of the calculations can be found in a paper dedicated to the dynamics of this system under publication.⁴⁵ The collisional cross sections are represented in Figure 5 for the transitions starting from the initial fundamental rotational and bending level of C₃. As can be seen on this figure the results of the dynamics obtained using the two models of PES are almost identical for collision energies larger than 1 cm⁻¹ which are of interest in astrochemistry.

V. CONCLUSIONS AND PERSPECTIVES

Generally, the comparison of the multidimensional PESs generated using the CCSD(T)-F12/aug-cc-pVTZ approach and the standard CCSD(T) method shows that we achieve similar accuracy over the intermonomer vdW coordinate. This method describes also correctly the region of the PESs involving these coordinates and the intra-monomer coordinate. Accordingly, the evolution of the potential along these coordinates is well account for in addition to the possible potential couplings. Nevertheless, the computational time (CPU) and disk space are reduced by up to two orders of magnitude when using CCSD(T)-F12 instead of standard CCSD(T).

In recent works, we showed that CCSD(T)-F12/aug-cc-pVTZ is the method of choice for the generation of 1D and 2D intermonomer long range potentials^{26,27,38} and 4D intermonomer polyatomic complexes.²⁸ Here, we go beyond these findings and a generalization is done. Indeed and through the comparison of the CCSD(T)-F12/aug-cc-pVTZ 4D-PES of C₃–He complex to the PESs generated using standard methodologies, we show that the use of explicitly correlated method leads to accurate mapping of the multi-dimensional PESs of polyatomic molecular systems, including the long range Jacobi and intermonomer coordinates and more interestingly the intramonomer degrees of freedom. As previously, a strong reduction of computational cost is observed. Hence, CCSD(T)-F12/aug-cc-pVTZ should be viewed as the key method for the generation of multi-dimensional polyatomic –He/H₂ potential energy surfaces for reactive and non-reactive collisions between polyatomic molecules (e.g., prebiotic molecules) with He or H₂, where several thousands (even millions) of energies for non-equivalent nuclear configurations are needed.

ACKNOWLEDGMENTS

This study was undertaken, while M.H. was a Visiting Professor at King Saud University. The support of the Visiting Professor Program at King Saud University is hereby gratefully acknowledged. O.D.-A., T.S., and P.H. thank a support from the Agence Nationale de la Recherche, Contract Nos. ANR-12-BS05-0011-01 and ANR-HYDRIDES. The authors acknowledge Marie Curie International Research Staff Exchange Scheme Fellowship within the 7th European

Community Framework Program under Grant No. PIRSES-GA-2012-31754 and the COST Action CM1002 CODECS.

- ¹I. Savic, I. Cermak, and D. Gerlich, *Int. J. Mass Spectrom.* **240**, 139 (2005).
- ²K. W. Hinkle, J. J. Keady, and P. F. Bernath, *Science* **241**, 1319 (1988).
- ³S. Saha and C. M. Western, *J. Chem. Phys.* **125**, 224307 (2006).
- ⁴A. Van Orden and R. Saykally, *J. Chem. Rev.* **98**, 2313 (1998).
- ⁵H. Fueno and Y. Taniguchi, *Chem. Phys. Lett.* **312**, 65 (1999).
- ⁶W. Weltner and R. J. Vanzee, *Chem. Rev.* **89**, 1713 (1989).
- ⁷See <http://webbook.nist.gov> for other previous experimental determinations.
- ⁸H. Hoshina, Y. Kato, Y. Morisawa, T. Wakabayashi, and T. Momose, *Chem. Phys.* **300**, 69 (2004).
- ⁹C. Jungen and A. J. Merer, *Mol. Phys.* **40**, 95 (1980).
- ¹⁰K. W. Chang and W. R. M. Graham, *J. Chem. Phys.* **77**, 4300 (1982).
- ¹¹G. Monninger, M. Forderer, P. Gurtler, S. Kalhofer, S. Petersen, L. Nemes, P. G. Szalay, and W. Kratschmer, *J. Phys. Chem. A* **106**, 5779 (2002).
- ¹²I. Cermak, M. Forderer, I. Cermakova, S. Kalhofer, H. Stopka-Ebeler, G. Monninger, and W. Kratschmer, *J. Chem. Phys.* **108**, 10129 (1998).
- ¹³H. Sasada, T. Amano, C. Jarman, and P. F. Bernath, *J. Chem. Phys.* **94**, 2401 (1991).
- ¹⁴D. W. Tokaryk and S. Civis, *J. Chem. Phys.* **103**, 3928 (1995).
- ¹⁵G. Q. Zhang, B. G. Lin, S. M. Wen, and Y. C. Hsu, *J. Chem. Phys.* **120**, 3189 (2004).
- ¹⁶K. Ahmed, G. G. Balint-Kurti, and C. M. Western, *J. Chem. Phys.* **121**, 10041 (2004).
- ¹⁷M. Mladenovic, S. Schmatz, and P. Botschwina, *J. Chem. Phys.* **101**, 5891 (1994).
- ¹⁸A. Terentyev, R. Scholz, M. Schreiber, and G. Seifert, *J. Chem. Phys.* **121**, 5767 (2004).
- ¹⁹F. Lique, R. Tobbya, J. Kyos, N. Feautrier, A. Spielfiedel, L. F. M. Vincent, G. Chayasiniski, and M. H. Alexander, *Astron. Astrophys.* **478**, 567 (2008).
- ²⁰T. R. Phillips, *MNRAS* **271**, 827 (1994); A. Faure, N. Crimier, C. Ceccarelli, P. Valiron, L. Wiesenfeld, and M. L. Dubernet, *Astron. Astrophys.* **472**, 1029 (2007).
- ²¹D. Ben Abdallah, K. Hammami, F. Najar, N. Jaidane, Z. Ben Lakhdar, M. L. Senent, G. Chambaud, and M. Hochlaf, *Astrophys. J.* **686**, 379 (2008).
- ²²C. A. Schmuttenmaer, R. C. Cohen, N. Pugliano, J. R. Heath, A. L. Cooks, K. L. Busarow, and R. J. Saykally, *Science* **249**, 897 (1990).
- ²³V. Spirko, M. Mengel, and P. Jensen, *J. Mol. Spectrosc.* **183**, 129 (1997).
- ²⁴G. Zhang, D. Zang, C. Sun, and D. Chen, *Mol. Phys.* **107**, 1541 (2009).
- ²⁵O. Denis-Alpizar, T. Stoecklin, and P. Halvick, *J. Chem. Phys.* **140**, 084316 (2014).
- ²⁶F. Lique, J. Klos, and M. Hochlaf, *Phys. Chem. Chem. Phys.* **12**, 15672 (2010).
- ²⁷Y. Ajili, K. Hammami, N. E. Jaidane, M. Lanza, Y. N. Kalugina, F. Lique, and M. Hochlaf, *Phys. Chem. Chem. Phys.* **15**, 10062 (2013).
- ²⁸Y. N. Kalugina, I. A. Buryak, Y. Ajili, A. A. Viginin, N. E. Jaidane, and M. Hochlaf, *J. Chem. Phys.* **140**, 234310 (2014).
- ²⁹H.-J. Werner, P. J. Knowles, G. Knizia, F. R. Manby, M. Schütz *et al.*, MOLPRO, version 2012.1, a package of *ab initio* programs 2012, see <http://www.molpro.net>.
- ³⁰T. H. Dunning, *J. Chem. Phys.* **90**, 1007 (1989).
- ³¹R. A. Kendall, T. H. Dunning, and R. J. Harrison, *J. Chem. Phys.* **96**, 6796 (1992).
- ³²W. Klopper, *Mol. Phys.* **99**, 481 (2001).
- ³³F. Weigend, A. Köhn, and C. Hättig, *J. Chem. Phys.* **116**, 3175 (2002).
- ³⁴M. O. Sinnokrot, E. F. Valeev, and C. D. Sherrill, *J. Am. Chem. Soc.* **124**, 10887 (2002).
- ³⁵O. Marchetti and H.-J. Werner, *J. Phys. Chem. A* **113**, 11580 (2009).
- ³⁶E. G. Hohenstein and C. D. Sherrill, *WIREs Comput. Mol. Sci.* **2**, 304–326 (2012).
- ³⁷G. Knizia, T. B. Adler, and H. Werner, *J. Chem. Phys.* **130**, 054104 (2009).
- ³⁸K. Mathivon, R. Linguetti, and M. Hochlaf, *J. Chem. Phys.* **139**, 164306 (2013).
- ³⁹O. Yazidi and M. Hochlaf, *Phys. Chem. Chem. Phys.* **15**, 10158 (2013).
- ⁴⁰M. Hochlaf, *Phys. Chem. Chem. Phys.* **15**, 9967 (2013).
- ⁴¹S. F. Boys and F. Bernardi, *Mol. Phys.* **19**, 553–566 (1970).
- ⁴²T. Stoecklin, O. Denis-Alpizar, P. Halvick, and M.-L. Dubernet, *J. Chem. Phys.* **139**, 124317 (2013).
- ⁴³J. M. Hutson and A. E. Thornley, *J. Chem. Phys.* **100**, 2505 (1994).
- ⁴⁴S. Carter, N. Handy, and B. Sutcliffe, *Mol. Phys.* **49**, 745 (1983).
- ⁴⁵O. Denis-Alpizar, T. Stoecklin, and P. Halvick, “Collision cross-section for excitation of C₃ by He” (unpublished).